

Operating an atom-interferometry-based gravity gradiometer by the dual-fringe-locking method

Xiao-Chun Duan, Min-Kang Zhou, De-Kai Mao, Hui-Bing Yao, Xiao-Bing Deng, Jun Luo, and Zhong-Kun Hu*

MOE Key Laboratory of Fundamental Physical Quantities Measurements, School of Physics, Huazhong University of Science and Technology, Wuhan 430074, People's Republic of China

(Received 21 April 2014; published 11 August 2014)

We report a gravity gradiometer composed of two atom interferometers which are simultaneously locked to the respective fringe center by feedback control of the Raman laser phase and magnetic field gradient. Compared with the conventional full-fringe recording method, this dual-fringe-locking strategy is capable of increasing the sampling rate and improving the sensitivity for gravity gradient measurements. Meanwhile, it retains the intrinsic advantage of rejecting common mode noises for gravity gradiometers. A short-term sensitivity of $670 \text{ E/Hz}^{1/2}$ with a 0.25 Hz sampling rate is achieved in our gravity gradiometer. This approach may also find possible applications in other atom-interferometry-based experiments utilizing dual atomic clouds.

DOI: [10.1103/PhysRevA.90.023617](https://doi.org/10.1103/PhysRevA.90.023617)

PACS number(s): 37.25.+k, 04.80.-y

I. INTRODUCTION

Atom-interferometry-based gravity gradiometers have been developed rapidly in recent years [1–7] and a sensitivity of about $30 \text{ E/Hz}^{1/2}$ has been achieved [2,4]. Important applications have been found in scientific and technical areas, ranging from measurements of the gravitational constant [8–14] and tests of general relativity [15–19] to the gravity gradient survey [20,21].

In the conventional operation of atom interferometers based on stimulated Raman transitions, the phase shift induced by Raman lasers is swept to record full interference fringes. However, the measurement data at the extremum points among one full fringe are less sensitive to phase variation than that at the midfringe, which will degrade the whole phase measurement sensitivity. In fact, the approach which allows measurements to be invariably performed at the fringe centers has already been adopted for atom gravimeters to improve the sensitivity [22–26], inspired by the work in atomic clocks [27]. In that fringe-locking approach, the Raman laser phase is no longer scanned step by step to sweep one full fringe. Instead, the Raman laser phase is modulated and then an error is obtained for feedback control of the phase to lock the interferometer at midfringe. This real-time feedback ensures that the measurements are always performed at the midfringes, whether or not there is a change of gravity acceleration or an external disturbance. Atom gravity gradiometers typically consist of two simultaneously operated atom interferometers. It is expected to also be advantageous to operate a gravity gradiometer by the fringe-locking method. However, it is difficult to simultaneously lock two atom interferometers with independent phase shifts at their most sensitive states through the Raman laser phase feedback alone. Here, by introducing an additional feedback control of the magnetic field gradient, we demonstrate an approach which ensures that the two atom interferometers always work simultaneously at the center of the respective fringe. With this dual-fringe-locking method, the measurement is more sensitive to the gravity gradient signal, and the measurement equations can be linearized at the same time, thus the differential phase shift is directly obtained for

every two launches. This measurement approach still retains the intrinsic advantage of rejecting common mode noises, and is also capable of increasing the sampling rate by about one order of magnitude and improving the sensitivity by about three times in our atom gravity gradiometer, as described in this paper.

II. THEORETICAL ANALYSIS

For an atom interferometer using stimulated Raman transitions [28], the transition probability P of the atoms following the $\pi/2 - \pi - \pi/2$ Raman pulses is [29–31]

$$P = A + D \cos(\Delta\varphi), \quad (1)$$

where A is the fringe offset, D is the fringe amplitude, and $\Delta\varphi$ is the total phase shift. For an ideal atom gravimeter, $\Delta\varphi = \alpha T^2 - \vec{k}_{\text{eff}} \cdot \vec{g} T^2$, where α is the chirp rate of the effective Raman laser frequency used to compensate the Doppler shift due to gravity, T is the separation time between the neighboring Raman pulses, and \vec{k}_{eff} is the effective wave number of Raman lasers. For clarity, the phase shift αT^2 is denoted as $\Delta\varphi_L$, and the second term $-\vec{k}_{\text{eff}} \cdot \vec{g} T^2$ is denoted as $\Delta\varphi_g$ here. In the conventional measurement procedure, full fringes are recorded by measuring P as a function of the controllable $\Delta\varphi_L$, and then the gravitational acceleration is obtained by the cosine fitting of the fringes. However, according to Eq. (1), $\delta P = -D \sin(\Delta\varphi) \delta(\Delta\varphi)$, we can know that the transition probability is least sensitive at the extremum points ($\Delta\varphi = n\pi$, where n is an integer) and is most sensitive at midfringe ($\Delta\varphi = n\pi + \pi/2$). In order to improve the performance, the measurement approach of locking the fringes in a single interferometer has already been adopted in atom gravimeters [22–26]. In the fringe-locking approach, the appropriate value of $\Delta\varphi_L$, denoted as $\Delta\varphi_L^0$, is found to make $\Delta\varphi \sim 2n\pi$. Then $\Delta\varphi_L$ is modulated by $\pm\pi/2$ with respect to the center of $\Delta\varphi_L^0$ so that the measurement is always performed at midfringe, alternately to the right and to the left side of the central fringe. From the difference between two consecutive measured transition probabilities, the phase error can be evaluated and then used to correct $\Delta\varphi_L^0$, from which the gravity acceleration can be obtained.

*zkhu@mail.hust.edu.cn

However, in gravity gradiometers consisting of two atom interferometers with different phase shifts, it is difficult to simultaneously lock the two fringes by exploring the Raman laser phase for feedback control alone. The phase shift induced by a magnetic field gradient has already been explored to change the differential phase shift in the atom gravity gradiometer (see Refs. [11,32], for example). Thus, in addition to using Raman laser phase feedback to lock one fringe, we can introduce a controllable magnetic field gradient to generate a phase shift to lock the other fringe. It is worth noting that since the phase shift induced by Raman lasers is the same for the two atom interferometers, what is necessary for this strategy to work is that the phase shifts between the two atom interferometers induced by the magnetic field gradient shall be different. With the phase shift induced by a magnetic field gradient included, the total phase shifts of the two interferometers can be expressed as $\Delta\varphi^{I,II} = \Delta\varphi_L + \Delta\varphi_g^{I,II} + \Delta\varphi_B^{I,II}$, where the superscript I,II denotes the upper and lower atom interferometer, respectively. In the simplest case when the changes of the magnetic-field-gradient-induced phase $\Delta\varphi_B^I$ and $\Delta\varphi_B^{II}$ are totally independent, the Raman-laser-induced phase $\Delta\varphi_L$ is thus controlled to lock one fringe, fringe II for example, while $\Delta\varphi_B^I$ is controlled to lock fringe I . The appropriate values of $\Delta\varphi_L$ and $\Delta\varphi_B^I$ are first found to make $\Delta\varphi^{I,II} \sim 2n^{I,II}\pi$ at the same time (both n^I and n^{II} are integers), and then the Raman laser phase is modulated by $\pm\pi/2$. In this case, the transition probabilities for the two atom interferometers for every two consecutive launches can be expressed as

$$\begin{cases} P_{2l}^{I,II} = A^{I,II} + D^{I,II} \cos(\Delta\varphi_L^0 + \Delta\varphi_g^{I,II} + \Delta\varphi_B^{I,II} - \pi/2) \\ P_{2l+1}^{I,II} = A^{I,II} + D^{I,II} \cos(\Delta\varphi_L^0 + \Delta\varphi_g^{I,II} + \Delta\varphi_B^{I,II} + \pi/2), \end{cases} \quad (2)$$

where the subscript l denotes the index of modulating cycles, and $\Delta\varphi_B^I$ temporarily stands for a certain appropriate value of $\Delta\varphi_B^I$ that assures $\Delta\varphi^I \sim 2n^I\pi$, which will be denoted as $\Delta\varphi_B^0$ hereafter. According to the linear approximation of Eq. (2) at midfringe, the correction can be expressed as

$$\begin{cases} \delta(\Delta\varphi_L^0) = (P_{2l+1}^{II} - P_{2l}^{II})/2D^{II} \\ \delta(\Delta\varphi_B^0) = (P_{2l+1}^I - P_{2l}^I)/2D^I - (P_{2l+1}^{II} - P_{2l}^{II})/2D^{II}. \end{cases} \quad (3)$$

Once the corrections are made to form a closed feedback loop, the equation $\Delta\varphi^{I,II} = 2n^{I,II}\pi$ is supposed to be tenable, from which $\Delta\varphi_g^I - \Delta\varphi_g^{II} = -(\Delta\varphi_B^0 - \Delta\varphi_B^{II}) + 2(n^I - n^{II})\pi$ can be deduced. Thus the value of the differential gravity acceleration can be obtained from the value of $\Delta\varphi_B^0$. It is shown in Eq. (3) that when the two atom interferometers are operated at the midfringes, the measurement works in a linear region and the differential phase shift of the gravity gradiometer can be directly obtained from $\Delta\varphi_B^0$ for every two consecutive launches. Equation (3) also implies that the common noises, such as Raman laser phase noise and vibration noise, only affect the correction of $\Delta\varphi_L^0$, while $\Delta\varphi_B^0$ is immune as long as the corresponding fluctuation is less than $\pi/2$. Compared with the conventional procedure, namely, recording full fringes and then exploring ellipse fitting [32] or Bayesian estimation [33,34], this linear measurement approach not only alleviates the effects of the data outlier, but

also improves the data rate and the sensitivity, while retaining the intrinsic advantage of rejecting common mode noise in gravity gradiometers.

III. EXPERIMENT

A. Experimental setup

The experimental setup of our atom interferometer, which is shown in Fig. 1, is almost the same as that described in Refs. [35–37]. It consists of a typical magnetic-optic trap (MOT) to load and launch atoms, a detection chamber, and an interference tube, with a vacuum at the level of 10^{-8} Pa. The Raman lasers, which are realized by phase locking two extended cavity diode lasers (ECDLs) using an optical phase locked loop (OPLL), are guided to the vacuum chamber from the top of the instrument and retroreflected by a mirror at the bottom. The mirror is fixed on an active vibration isolator to reduce the influence of vibration noise, which has been presented in detail in Refs. [25,37]. While this instrument is originally built up for gravity measurements in our laboratory [37,38], it can also be used for gravity gradiometer measurements by consecutively launching two clouds of atoms to different heights from a single MOT, inspired by the work in Refs. [9–13]. By precisely controlling the launch velocities and the time separation between launches, the two clouds of atoms, denoted as cloud I and cloud II , respectively, in Fig. 1, remain separated by a near constant distance of 0.45 m throughout their free fall. The time delay between the two launches, which allows the loading of cloud II , is only about 100 ms. To increase the atom number in cloud II , a juggling method is adopted [39]. A cloud of atoms is first loaded and prelaunched to 0.7 m above the MOT; during its ballistic flight, cloud I is loaded and then launched to 1.15 m;

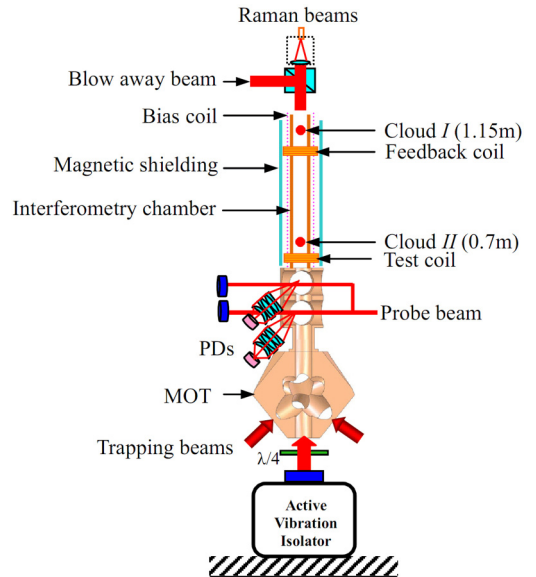


FIG. 1. (Color online) Schematic of the experimental setup. The two atomic clouds are freely falling with almost the same velocity at different heights. The feedback coil used for locking fringe I is close to the apogee of cloud I , while the test coil used to induce an additional phase shift for the test is close to the apogee of cloud II .

finally, the prelaunched cloud of atoms returns to the MOT and is recaptured, which is then launched to 0.7 m to form cloud *II*. The temperature of the atoms is about 7 μ K, and the detected number of atoms in the two clouds when they fall back into the detection chamber is about 10^7 without state preparation. When both of the atomic clouds enter the magnetic shielding zone, a Raman π pulse with a duration of 22 μ s is applied to select the atoms in the magnetic-insensitive state $|F = 1, m_F = 0\rangle$ and in a narrow region of vertical velocity distribution simultaneously for both atomic clouds. The quantization axis along the vertical direction is set by a magnetic field of about 275 mG, which is produced by the bias coil with a current of 25 mA. After the unwanted atoms are removed by a blow-away beam, the two atomic clouds simultaneously undergo the $\pi/2 - \pi - \pi/2$ Raman pulses, where the separation time T between pulses is 165 ms. Finally, the transition probabilities of the two atomic clouds are sequentially obtained through a normalized fluorescence detection when the corresponding atomic cloud falls back into the detection chamber. The entire process of a single shot measurement as described above takes 2 seconds.

B. Phase shift induced by the feedback coil

The adjustment of the magnetic-field-gradient-induced phase shift is realized by controlling the current through an additional coil, denoted as the feedback coil, as shown in Fig. 1. This feedback coil is wrapped between the bias coil and the magnetic shielding, with a length of tens of loops and a distance of about 50 mm below the apogee of cloud *I* and about 400 mm above the apogee of cloud *II*. With such a configuration, we can expect that the influence of the feedback coil on cloud *II* is negligible, while the corresponding induced phase shift for cloud *I* is dominant. In the fringe-locking mode, the current of the feedback coil is always on and keeps constant in each shot to produce a time-invariable but spatially inhomogeneous magnetic field during the whole interfering procedure. However, in our experiment, the interfering π pulse moment is about a 6 ms delay after the apogee moment. Thus, for the two pulses' separations, there are 12 ms durations for which the atoms experience different magnetic field, as a result of the flight asymmetry during the two pulses' separations. For a rough estimation, a magnetic field difference of about 40 mG induced by the feedback coil between the apogee zone and the zone where the third interfering pulse is applied will cause an additional 1 rad phase shift for cloud *I*. In practice, the phase shift of the two atom interferometers induced by the feedback coil is measured experimentally by recording full fringes simultaneously for both atom interferometers in different injected currents. In the calibration experiment of the feedback coil, the chirp rate α is scanned in 20 steps to get one full fringe. Meanwhile, in order to reduce the influence of the gravity tidal effect, the data of every two adjacent fringes are combined to make a differential measurement. For one fringe, the feedback coil is injected with an interested value, and for the other fringe, the feedback coil current is zero. The result is shown in Fig. 2, where every point is an average of 60 consecutive differential measurements. It is clearly shown that the phase shift of cloud *I* induced by the feedback coil follows a quadratic polynomial relation as expected, and the

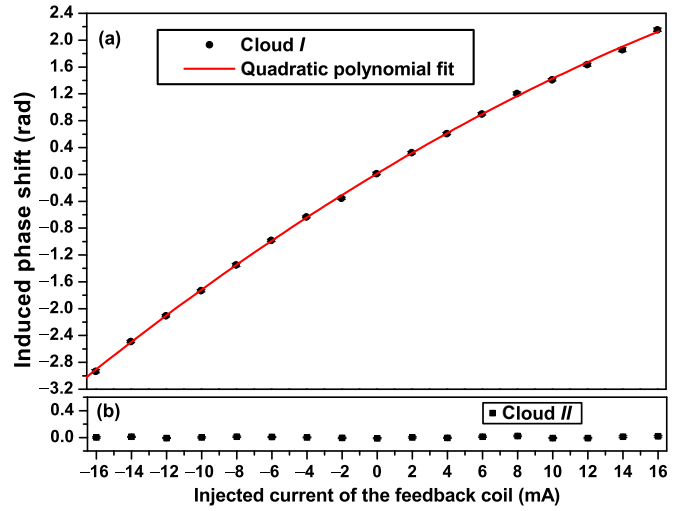


FIG. 2. (Color online) The induced phase shift by the feedback coil at different values of injected current, with (a) for cloud *I* and (b) for cloud *II*.

influence of the magnetic field gradient generated by the feedback coil on cloud *II* can be neglected [the corresponding standard deviation of the data as shown in Fig. 2(b) is about 3 mrad]. According to the quadratic polynomial fitting result, the magnetic-field-gradient-induced phase shift for cloud *I* can be expressed as

$$\frac{(\Delta\varphi_B^I)_f}{1 \text{ mrad}} = 6(6) + 157.3(5) \times \frac{I_f}{1 \text{ mA}} - 1.57(6) \left(\frac{I_f}{1 \text{ mA}} \right)^2, \quad (4)$$

where I_f is the feedback coil current. By combining Eqs. (3) and (4), we can obtain the correction of the injected current, which can then serve as feedback to the current source meter (Agilent B2902A). Finally, by automatically controlling the chirp rate and the injected current via the computer, the corrections of $\Delta\varphi_L^0$ and $\Delta\varphi_B^0$ can be realized to simultaneously lock the two interferometers to the respective fringe center.

C. Gravity gradiometer operation

Before locking the fringes, the full fringes are recorded by sweeping the chirp rate and the cosine fitting is performed to obtain the fringe amplitude $D^{I,II}$ and the phase shifts of the two interferometers, from which the initial appropriate values of $\Delta\varphi_L$ and $\Delta\varphi_B$ are estimated. Typically, 20 full fringes are recorded in our experiment to get an initial estimation of $\Delta\varphi_L^0$ and $\Delta\varphi_B^0$. It then automatically switches to the fringe-locking mode, as shown in Fig. 3. It is clearly shown that the interferometers are simultaneously operated at the center of the respective fringe in the fringe-locking mode.

In this demonstration, for every two launches, the corrections are made exactly according to Eq. (3) without any tunable parameters. It is expected that in this way, the noise and external disturbance of the instrument can be faithfully reflected. For each correction, the current for the feedback coil is corrected at the beginning of the atoms' loading procedure, which assures enough time for the possible eddy current to damp before the interference procedure. From the recorded

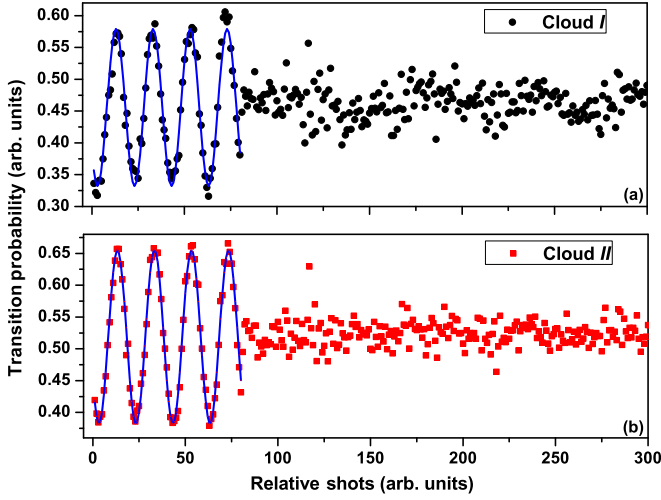


FIG. 3. (Color online) The switch between full-fringe recording mode and fringe-locking mode, with (a) for cloud *I* and (b) for cloud *II*, respectively. The solid line in each picture is a sinusoidal fit of the experimental points for each cloud.

feedback coil current, the variation of the differential phase shift of the two atom interferometers is obtained using Eq. (4). In our experiment, the current of the feedback coil jumps from zero to about 1.4 mA during the switch between the two modes. And the correction of the feedback coil current is less than 1 mA in the fringe-locking mode for our gravity gradiometer measurement, which is supposed to be mainly caused by the noise in the measurement (the stability of the current source meter is better than $1\ \mu\text{A}$ in a range of 100 mA, of which the influence can be neglected at the noise level of this work). The corresponding performance can be evaluated using the Allan deviation, as shown in Fig. 4. The Allan deviation of the gravity gradiometer operated in the full-fringe recording mode

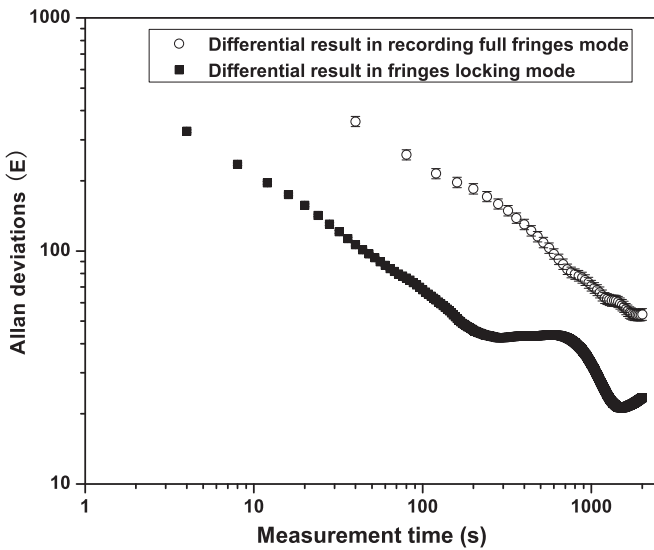


FIG. 4. The performances characterized by Allan deviation. The Allan deviation of the gravity gradient measurement in the full-fringe recording mode is displayed as open circles, and the one in the fringe-locking mode is displayed as solid squares.

is also shown as the open circles in Fig. 4. It is clearly shown that the short-term sensitivity of the gravity gradiometer in the fringe-locking mode has been improved, in our case by about three times compared with that in the full-fringe recording mode. Meanwhile, the sampling rate increases from 0.025 to 0.25 Hz, an improvement of one order of magnitude. The short-term sensitivity for the gravity gradient measurement in the fringe-locking mode is about $670\ \text{E}/\text{Hz}^{1/2}$ according to the Allan deviation data as shown in Fig. 4. There is a room-temperature fluctuation in our experiments, which may account for the bump in the Allan deviation at about 1000 s, as shown in Fig. 4.

The resolution of our gravity gradiometer can be further confirmed by measuring an additional gravitational gradient produced by well-machined source masses. Four stainless steel SS316 spheres are symmetrically placed around the interferometry tube. The centers of the spheres are $(73 \pm 5)\ \text{mm}$ below the mean height of the apexes of the two clouds with a horizontal distance of $(110 \pm 5)\ \text{mm}$ from the symmetrical axis of the interferometry tube. All four spheres are selected from the same batch of source masses that was used for measuring G in our cave laboratory. Each mass is about 8.55 kg. The theoretical effective mean gravitational gradient produced by these four spheres is $(157 \pm 6)\ \text{E}$. The source masses are manually taken on and off periodically, and the corresponding change is measured by our gravity gradiometer, as shown in Fig. 5. The black squares represent the measured gravity gradient when the four spheres are placed at the positions as described above (masses on), and the red dots represent the results without the source masses (masses off). Each point in Fig. 5 is an average of 25 measurements within 100 s. It is shown that the standard deviation of each point is about 70 E, which is consistent with the Allan deviation in Fig. 4. The mean variation between the cases of masses on and off in Fig. 5 is $(146 \pm 16)\ \text{E}$ (the uncertainty is the standard deviation of the mean variation from the statistics on the data as shown

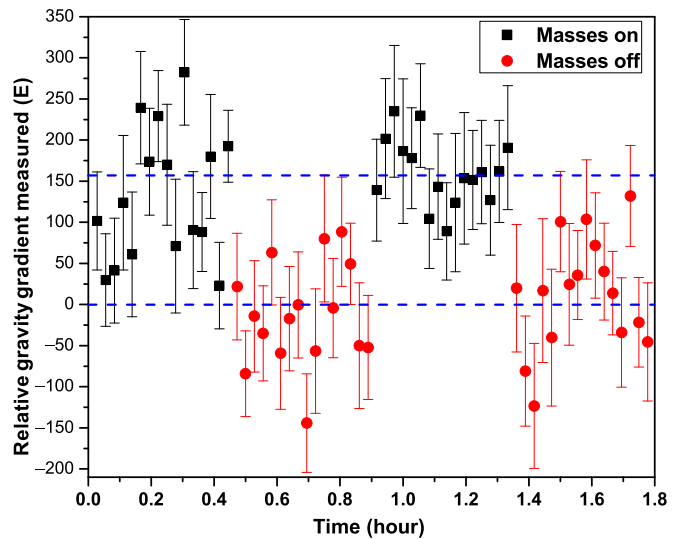


FIG. 5. (Color online) The measured variation between the cases of taking masses on and off by our gravity gradiometer. The two dashed lines indicate the theoretical variation.

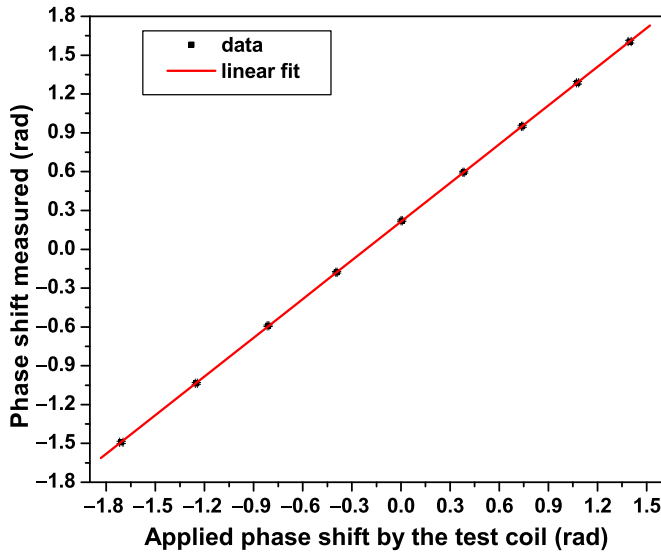


FIG. 6. (Color online) The result of the validation experiment. The measured phase shift is induced by the current of the feedback coil according to Eq. (4).

in Fig. 5), which also agrees with the theoretically calculated value (157 ± 6) E.

D. Approach validation

To further validate this approach, a second coil, denoted as the test coil in Fig. 1, is explored to change the differential phase shift between the two atom interferometers. The differential phase shift due to the test coil at different injected current is measured by recording full fringes of the two atom interferometers, just like the calibration of the feedback coil. Then different currents are injected into the test coil in turn when the gravity gradiometer is operated in the fringe-locking mode, and the corresponding response of the feedback coil current is recorded, from which the change of the differential phase shift between the two atom interferometers can be obtained, as shown in Fig. 6. According to the result of the linear fitting in Fig. 6, the slope 0.997(1) is very close to the expected value of 1, and the intercept 0.214(1) rad is compatible with the measured differential phase shift 0.210(3) rad when the gravity gradiometer is working in the full-fringe recording mode without an injected current for either the feedback coil or the test coil. This principle experiment confirms the effectiveness of the fringe-locking approach in tracking the change of the differential phase shift of the gravity gradiometer with a range of 2π .

IV. DISCUSSION AND CONCLUSION

In our experiment, the dominant noise probably comes from the technical detection noise, which is still under investigation. We can expect an improvement of our gravity gradiometer by increasing the atom number and decreasing the temperature of the atomic clouds further. In experiments where the technical detection noise is not dominant, the data rate and the short-term sensitivity are still expected to be improved using this dual-fringe-locking method. Based on the idea that utilizes two quantities for feedback control to lock two fringes, this approach may also find possible applications in other atom-interferometry-based experiments utilizing dual atomic clouds, for example, the atom gyroscopes [40–42]. The fringe-locking approach is sensitive to the drift of the fringe amplitude, which can be resolved by occasionally switching back to the full-fringe recording mode to get a renewed fringe amplitude. It also must be noted that this approach is fragile with obvious common mode noises and is more sensitive to the jitter of the cloud position than the conventional approach for the introduction of an additional magnetic field gradient. However, these drawbacks can be alleviated by the stabilization of the system and suppression of the common mode noises. At last, we note that an eddy current induced by the correction of the feedback coil current may be an obstacle in high data rate measurements. However, it is supposed to be innocuous in the usual precision measurements by atom interferometry, where the atom loading time typically exceeds 100 ms.

In conclusion, we have demonstrated a dual-fringe-locking approach for an atom-interferometry-based gravity gradiometer, where the two atom interferometers are simultaneously operated at the fringes' center. With this fringe-locking approach, a short-term sensitivity of about $670 \text{ E/Hz}^{1/2}$ with a sampling rate of 0.25 Hz has been achieved in our atom gravity gradiometer. Compared with the conventional measurement procedure, this approach is capable of improving both the data rate and the sensitivity for gravity gradient measurement. Since this approach can be easily implemented, it can be adopted in related experiments exploring dual atomic clouds, for example, measuring the gravitational constant and the rotation of the Earth, to improve the corresponding performance.

ACKNOWLEDGMENTS

We thank Zehuang Lu, Xianji Ye, and Chenggang Shao for enlightening discussions. This work is supported by the National Natural Science Foundation of China (Grants No. 41127002, No. 11204094, and No. 11205046) and the National Basic Research Program of China (Grant No. 2010CB832806).

- [1] M. J. Snadden, J. M. McGuirk, P. Bouyer, K. G. Haritos, and M. A. Kasevich, *Phys. Rev. Lett.* **81**, 971 (1998).
- [2] J. M. McGuirk, G. T. Foster, J. B. Fixler, M. J. Snadden, and M. A. Kasevich, *Phys. Rev. A* **65**, 033608 (2002).

- [3] F. Sorrentino, Q. Bodart, L. Cacciapuoti, Y. H. Lien, M. Prevedelli, G. Rosi, L. Salvi, and G. M. Tino, *Phys. Rev. A* **89**, 023607 (2014).
- [4] N. Yu, J. M. Kohel, J. R. Kellogg, and L. Maleki, *Appl. Phys. B* **84**, 647 (2006).

- [5] F. Sorrentino, A. Bertoldi, Q. Bodart *et al.*, *Appl. Phys. Lett.* **101**, 114106 (2012).
- [6] P. A. Altin, M. T. Johnsson, V. Negnevitsky *et al.*, *New J. Phys.* **15**, 023009 (2013).
- [7] Y. Bidel, O. Carraz, R. Charrière, M. Cadoret, and N. Zahzam, *Appl. Phys. Lett.* **102**, 144107 (2013).
- [8] J. B. Fixler, G. T. Foster, J. M. McGuirk, and M. A. Kasevich, *Science* **315**, 74 (2007).
- [9] G. Lamporesi, A. Bertoldi, L. Cacciapuoti, M. Prevedelli, and G. M. Tino, *Phys. Rev. Lett.* **100**, 050801 (2008).
- [10] J. Stuhler, M. Fattori, T. Petelski, and G. M. Tino, *J. Opt. B: Quantum Semiclass. Opt.* **5**, S75 (2003).
- [11] A. Bertoldi, G. Lamporesi, L. Cacciapuoti *et al.*, *Eur. Phys. J. D* **40**, 271 (2006).
- [12] F. Sorrentino, Y. H. Lien, G. Rosi, L. Cacciapuoti, M. Prevedelli, and G. M. Tino, *New J. Phys.* **12**, 095009 (2010).
- [13] M. Fattori, G. Lamporesi, T. Petelski, J. Stuhler, and G. M. Tino, *Phys. Lett. A* **318**, 184 (2003).
- [14] G. Rosi, F. Sorrentino, L. Cacciapuoti, M. Prevedelli, and T. M. Tino, *Nature (London)* **510**, 518 (2014).
- [15] S. Dimopoulos, P. W. Graham, J. M. Hogan, M. A. Kasevich, and S. Rajendran, *Phys. Rev. D* **78**, 122002 (2008).
- [16] S. Dimopoulos, P. W. Graham, J. M. Hogan, and M. A. Kasevich, *Phys. Rev. Lett.* **98**, 111102 (2007).
- [17] A. Bonnain, N. Zahzam, Y. Bidel, and A. Bresson, *Phys. Rev. A* **88**, 043615 (2013).
- [18] N. Gaaloul, H. Ahlers, T. A. Schulze *et al.*, *Acta Astronaut.* **67**, 1059 (2010).
- [19] S. Dimopoulos, P. W. Graham, J. M. Hogan, M. A. Kasevich, and S. Rajendran, *Phys. Lett. B* **678**, 37 (2009).
- [20] L. Maleki, N. Yu and J. Kohel, *AIAA Space 2004 Conference and Exhibit* (2004), doi:10.2514/6.2004-5906.
- [21] X. Wu, Ph.D. thesis, Stanford University, 2009.
- [22] P. Cheinet, F. P. Dos Santos, T. Petelski *et al.*, *Appl. Phys. B* **84**, 643 (2006).
- [23] J. Le Gouët, T. E. Mehlstäubler, J. Kim *et al.*, *Appl. Phys. B* **92**, 133 (2008).
- [24] S. Merlet, J. Le Gouët, Q. Bodart *et al.*, *Metrologia* **46**, 87 (2009).
- [25] Z. K. Hu, B. L. Sun, X. C. Duan, M. K. Zhou, L. L. Chen, S. Zhan, Q. Z. Zhang, and J. Luo, *Phys. Rev. A* **88**, 043610 (2013).
- [26] M. K. Zhou, B. Pelle, A. Hilico, and F. PereiradosSantos, *Phys. Rev. A* **88**, 013604 (2013).
- [27] A. Clairon, P. Laurent, G. Santarelli *et al.*, *IEEE Trans. Instrum.* **44**, 128 (1995).
- [28] M. Kasevich and S. Chu, *Phys. Rev. Lett.* **67**, 181 (1991).
- [29] M. Kasevich and S. Chu, *Appl. Phys. B* **54**, 321 (1992).
- [30] A. Peters, K. Y. Chung, and S. Chu, *Metrologia* **38**, 25 (2001).
- [31] Ch. J. Bordé, *Metrologia* **39**, 435 (2002).
- [32] G. T. Foster, J. B. Fixler, J. M. McGuirk, and M. A. Kasevich, *Opt. Lett.* **27**, 951 (2002).
- [33] J. K. Stockton, Xinan Wu, and M. A. Kasevich, *Phys. Rev. A* **76**, 033613 (2007).
- [34] G. Varoquaux, R. A. Nyman, R. Geiger *et al.*, *New J. Phys.* **11**, 113010 (2009).
- [35] M. K. Zhou, Z. K. Hu, X. C. Duan, B. L. Sun, J. B. Zhao, and J. Luo, *Phys. Rev. A* **82**, 061602(R) (2010).
- [36] Z. K. Hu, X. C. Duan, M. K. Zhou, B. L. Sun, J. B. Zhao, M. M. Huang, and J. Luo, *Phys. Rev. A* **84**, 013620 (2011).
- [37] M. K. Zhou, Z. K. Hu, X. C. Duan, B. L. Sun, L. L. Chen, Q. Z. Zhang, and J. Luo, *Phys. Rev. A* **86**, 043630 (2012).
- [38] M. K. Zhou, Z. K. Hu, X. C. Duan *et al.*, *Front. Phys. China* **4**, 170 (2009).
- [39] R. Legere and Kurt Gibble, *Phys. Rev. Lett.* **81**, 5780 (1998).
- [40] B. Canuel, F. Leduc, D. Holleville *et al.*, *Phys. Rev. Lett.* **97**, 010402 (2006).
- [41] A. Gauguier, B. Canuel, T. Lévêque, W. Chaibi, and A. Landragin, *Phys. Rev. A* **80**, 063604 (2009).
- [42] T. Müller, M. Gilowski, M. Zaiser *et al.*, *Eur. Phys. J. D* **53**, 273 (2009).